

PHYSICAL REVIEW A

ATOMIC, MOLECULAR, AND OPTICAL PHYSICS

THIRD SERIES, VOLUME 47, NUMBER 6

JUNE 1993

RAPID COMMUNICATIONS

The Rapid Communications section is intended for the accelerated publication of important new results. Since manuscripts submitted to this section are given priority treatment both in the editorial office and in production, authors should explain in their submittal letter why the work justifies this special handling. A Rapid Communication should be no longer than 4 printed pages and must be accompanied by an abstract. Page proofs are sent to authors.

Strong onset of ionization in slow Xe^{q+} -Xe collisions at very high q

H. Cederquist, C. Biedermann, N. Selberg, E. Beebe, M. Pajek,* and A. Bárány

Manne Siegbahn Institute of Physics, S-104 05 Stockholm, Sweden

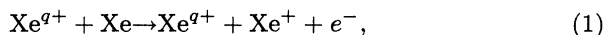
(Received 2 December 1992)

We have discovered that ionization without accompanying electron capture is an important process in slow ($v \sim 0.1$ – 0.2 a.u.) Xe^{q+} -Xe collisions at very high projectile charge ($q > 25$). The measured absolute cross sections, although between one and two orders of magnitude lower than the ones for single-electron capture, increase rapidly with q when $q > 25$ and reach a level of $\sim 1 \times 10^{-15}$ cm² for $q > 30$. We argue that the reaction mechanism for ionization of the heavier rare gases involves the formation of core-excited, autoionizing, neutral target states.

Pacs number(s): 34.70.+e, 34.50.Fa

For more than half a century it has been known that electron capture and ionization compete in fast ion-atom collisions [1]. In slow collisions, though, electron capture is expected to dominate strongly over ionization, since the total energy of each active electron is negative with respect to the projectile at internuclear distances where electrons can be released from the target [2, 3]. Emission of electrons during slow collisions of highly charged ions with multielectron targets is therefore usually mediated by electron capture; i.e., transfer ionization is a dominating ionization process [4].

In this Rapid Communication we report on experimental evidence for ionization *without* accompanying electron capture in slow collisions involving projectiles of very high charge. Absolute cross sections σ_I are found to be in excess of 1×10^{-15} cm² for the collisions



with $q > 30$ at $v = 0.034\sqrt{q}$ a.u. This is very surprising, at least at a first glance, since the velocities are about ten times lower than the classical Bohr-Lindhard limit for ionization [2] $v_{\min} = q^{1/4}\sqrt{I_1}$. In Fig. 1 we show absolute cross sections for the pure ionization process (1). Note, however, that even though the ionization cross section exhibits a threshold at $q = 13 \pm 3$ and follows an approximate q^2 behavior at higher q , it is about two orders of magnitude smaller than the sum of all capture cross sections for each q investigated here ($15 \leq q \leq 37$) [5].

In order to explain these results we propose a mechanism in which an electron is dynamically transferred to a Rydberg state of the projectile while, at the same time, the fine structure of the lowest Xe^+ term is excited.

The Rydberg electron may then be transferred back to form a core-excited neutral state, which readily autoionizes. This model will be accounted for in more detail below. First, however, we will discuss the experimental technique.

A 90% enriched ^{136}Xe gas was injected into the cryogenic electron-beam ion source at the Manne Siegbahn Institute of Physics [6]. The pressure in the ~ 6.5 -m-long transport line between the source and the entrance slits

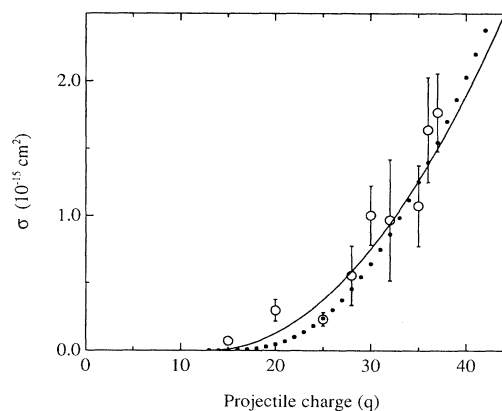


FIG. 1. Absolute experimental cross sections (open circles) for ionization in Xe^{q+} -Xe collisions as a function of q at $v = 0.034\sqrt{q}$ a.u. The error bars consist of statistical errors and uncertainties in the background subtraction. The full line shows a least-squares fit to the experimental data. The dotted line is the model cross section multiplied by a factor of 4 (cf. text).

of the separator magnet was 1×10^{-8} Torr. After charge-state selection, the beam propagated ~ 1.5 m at a pressure of about 5×10^{-9} Torr before entering a collision gas cell. We used a position-sensitive detector in order to register the final charge states of highly charged Xe ions after their passage through a 160° electrostatic hemispherical energy analyzer. The recoil ions were extracted from the gas cell by a weak electric field and their charge states were determined by means of a time-of-flight spectrometer. This technique is widely used, and details of this specific version were recently accounted for [4].

The pressure in the gas cell, which had an effective length of 10 mm, was measured by means of a capacitance manometer. No significant variation in the ratio between single ionization and single-electron capture between 0.06 and 0.33 mTorr was found for Xe^{32+} -Xe collisions. This strongly indicates that the dominating double-collision effect on the ionization peak is the same as the one for capture; namely, a reduction due to secondary capture events. The single-collision conditions are thus well established.

The principal quantum number n of the projectile capture state increases with the projectile charge and is expected [7] to be around 17 for Xe^{30+} -Xe collisions. The stripping of a captured electron could, in principle, give rise to false coincidences in the ionization spectra. We argue, though, that stripping of the comparatively large $\text{Xe}^{(q-1)+}$ state through interactions with the residual gas, the exit apertures or electric fields are equally unlikely. Residual gas stripping can be ruled out, since stripping in the target gas with two orders of magnitude greater thickness has been shown to be unimportant above. The main effect arising from interactions with the exit aperture is the capture of electrons, which for the case of Xe^{30+} projectiles will take place at a distance outside the surface, which is much larger than the Xe^{29+} ($n=17$) state before relaxation (~ 10 a.u.). Ionization by the 50-V/mm extraction field in the gas cell will only affect [8] states with $n > 430$. Further, the binding energy of the active electron increases considerably as it is transferred from the Xe atom ($I_1 \sim 12$ eV) to the $n=17$ state of Xe^{29+} (~ 42 eV).

Metastable projectiles may, after the capture of one electron, form a doubly excited state with sufficient energy for autoionization. This can then give rise to a false ionization signal [9, 10], as has been observed in the region $q \sim 10$. Although we do not have direct experimental proof that this does not occur, we consider it to be highly unlikely for the following reasons. (i) The probabilities [11] for forbidden transitions scale as q^m , where m is at least 6. For $q=30$, e.g., this means that the lifetime of a metastable state is $\sim 10^9$ times shorter than the lifetime of the isoelectronic state in the neutral atom and can hence be expected to be much shorter than the $20 \mu\text{s}$ it takes for the Xe^{30+} projectile to reach the gas cell. (ii) The measured ionization cross section increases monotonically with q . If the corresponding signal would be due to metastable projectiles, strong variations as a function of q would be expected due to differences in metastable fractions for different q [9, 10].

In Fig. 2(a), we show a projection of a two-dimensional

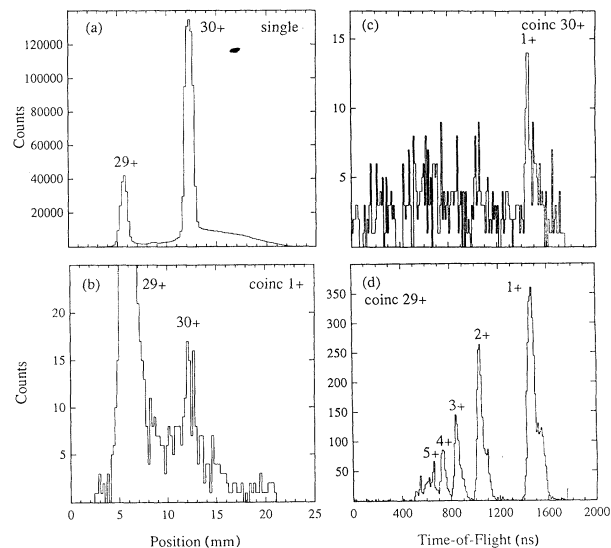


FIG. 2. Charge-state distributions of projectile and recoil ions from the target following Xe^{30+} -Xe collisions at $v=0.18$ a.u. A projection of the total two-dimensional spectrum on the axis of charge-state dispersion (a). (b) shows the same spectrum for events where a Xe^+ recoil ion was detected in coincidence. Time-of-flight spectra coincident with Xe^{30+} and Xe^{29+} are shown in (c) and (d), respectively. The weak structures superimposed on the random coincidence background in the range 300–900 ns are due to ionization of the residual gas (mainly CO_2 , O_2 , N_2 , and H_2O).

detector image on the axis of charge-state dispersion for Xe^{30+} -Xe collisions. In Fig. 2(b), the same projection is shown for projectiles coincident with singly charged recoil ions. The time-of-flight distributions coincident with Xe^{30+} and Xe^{29+} are shown in Figs. 2(c) and 2(d), respectively. The background in Fig. 2(c), is mainly due to random coincidences between recoil ions and Xe^{30+} projectiles, and will appear at the primary beam in the position spectrum. In order to handle this problem, the beam pulses were extended to ~ 50 ms and Xe^{q+} intensities were limited to ~ 100 per pulse during the measurements. With the time-to-amplitude converter open for $2 \mu\text{s}$ and with an evenly distributed intensity in the beam pulse, this gives an expected random coincidence probability of about 0.004 per detected recoil ion, which should be compared with an ionization probability of ~ 0.01 per detected recoil ion. Since the time-of-flight peak for the “1+” recoil is about 200 ns wide at the base, only one-tenth of the random coincidences in Fig. 2(c) (distributed over $2 \mu\text{s}$) are expected to show up at the “30+” position in Fig. 2(c). The ratio of true to random events in the peak for Xe^{30+} projectiles gated on singly charged recoil ions [Fig. 2(b)] is thus estimated to be $0.01/(0.004/10)=25$. Some caution is, however, still called for, since we cannot exclude higher concentrations of projectile ions in part of the pulse, and we deduce a true to random event ratio of ~ 10 from Fig. 2(c). A further problem is that electrons produced by Xe^{29+} at a mesh directly in front of the detector lead to a sloping background below the “30+” peak of Fig. 2(b). Note, however, that this tail of the “29+” peak

gives a time-of-flight spectrum identical to that of single-electron capture. For assignment of a single-ionization process we demand that the data exhibit the following features: (i) a peak of the right position and width in the projectile position spectrum coincident with a “1+” recoil ion; (ii) a peak of the right position and width in the time-of-flight spectrum coincident with projectiles of conserved charge; (iii) a recoil ion distribution coincident with Xe^{q+} that should be different from the one coincident with $\text{Xe}^{(q-1)+}$.

The ionization cross sections are determined by fitting Gaussian functions to the peaks corresponding to single-electron capture and single ionization. An absolute cross section for the latter process was determined through the ratio between these two processes and single-electron capture cross sections reported earlier [5]. The ionization cross section in Fig. 1 increases approximately as q^2 , and has an onset at about $q=13$. The full line shows a least-squares fit to the experimental data with the functional form $\sigma_I = a(q-b)^c$, where $a = (2.4 \pm 0.6) \times 10^{-18} \text{ cm}^2$, $b = 13 \pm 3$, and $c = 1.8 \pm 0.2$. Ionization without accompanying electron capture, on the level of a few percent of single-electron capture (first announced in [5]), has very recently also been found for $\text{Kr}^{25+}\text{-Ar}$ [12] and $\text{Ar}^{16+}\text{-He}$ [13] collisions at somewhat higher velocities.

In order to get a better perspective of the presently observed phenomenon we first consider some one-electron models. Using the dipole approximation for the ion-atom interaction, Janev and Presnyakov [14] arrived at an expression for ionization in the adiabatic region. From their formula we get an ionization cross section of only $\sim 3q \times 10^{-24} \text{ cm}^2$ for $\text{Xe}^{q+}\text{-Xe}$ collisions at $v = 0.034\sqrt{q}$ a.u. by using the effective oscillator strength for hydrogen (which has about the same ionization potential as Xe) and taking the six valence electrons of Xe into account. This one-electron model thus does not seem to be applicable in our case.

Two other ionization mechanisms have been discussed recently [15]. They are predicted to scale with q for high q and are associated with two different barrier-ionization processes. When the projectile and the target separate after the collision, an active electron residing close to the top of the internuclear potential barrier may be sequentially promoted to higher-lying quasimolecular states until ionization occurs. This mechanism is predicted to contribute on a level of about 10^{-20} cm^2 for a bare nucleus of charge $q=30$ colliding on atomic hydrogen [15]. The second mechanism, which involves ionization by an effective barrier connecting to the centrifugal barrier in the united atom limit, is predicted [15] to give substantially larger cross sections of about 10^{-17} cm^2 . This cross section includes contributions from electron capture to the continuum of the projectile. Electron capture to bound projectile states is, however, a strongly dominating process at all impact parameters, and it is hard to imagine that the centrifugal-barrier ionization mechanism, which occurs at relatively small impact parameters, could proceed without accompanying electron capture (to bound states) at large internuclear separations. Thus neither one of these one-electron models is able to explain the present observation.

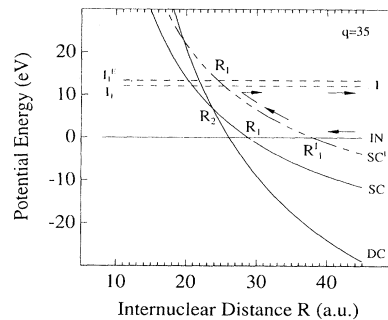


FIG. 3. A schematic of some diabatic potential-energy curves for $\text{Xe}^{35+}\text{-Xe}$ collisions. The initial channel is denoted by IN, while the single- and double-electron capture curves predicted to be active by the extended classical-over-the-barrier model are denoted by SC and DC, respectively. R_1 and R_2 are the internuclear distances at which the first and the second electrons are classically allowed to transfer to the projectile. Autoionizing core-excited neutral Xe states reside between the two lowest ionization levels, I_1 ($=12.10 \text{ eV}$) and I_1^E ($=13.33 \text{ eV}$), of Xe. An electron transferred to a single-capture channel SC^I at R_I^I interacts with the core-excited neutral channels at $R_I > R_2$. The reaction path is indicated by the arrows (cf. text).

Instead, we suggest a mechanism, indicated in Fig. 3, to be responsible for the unexpectedly large ionization cross sections. In a first step, one electron is transferred to the projectile at an internuclear separation R_I^I , slightly larger than the distance R_1 at which the outermost target electron is captured according to the classical over-the-barrier model [16, 17]. The probability of following the adiabatic path on the way to the radial turning point is calculated by means of a modified form of a semiempirical expression for the adiabatic energy splitting [18]. The modification is chosen in such a way that the maximum of the reaction window for single-electron capture, calculated by means of the Landau-Zener model, coincides with R_1 . This modification is supported by the excellent agreement [9, 19, 20] between experimental observations of the n distributions of projectile capture states and n values expected to be populated when the electron is transferred at R_1 . The radial velocity at R_1^I will be comparatively high, since b has to be smaller than the internuclear distance R_I , where the dashed single-capture channel cross with channels where core-excited states of neutral Xe are populated (cf. Fig. 3). The probability of following the adiabatic path at R_1^I , which is on the diabatic side of the reaction window, is thus found to be typically a few percent. For $\text{Xe}^{35+}\text{-Xe}$ collisions R_I^I/R_1 must be larger than 1.20 in order for the crossing at R_I^I to be outside the internuclear distance R_2 . For smaller R_I^I (and hence b) a second electron becomes quasimolecular, which is expected to drastically decrease the probability of exiting the collision without capture of at least one electron. The restriction $R_I > R_2$ implies that a projectile n state, slightly higher than the one populated at R_1 , is populated at R_1^I . Corresponding widths of n -state populations are expected from dynamical considerations [17] and have been observed experimentally [9, 19, 20].

The target may be left in either a $\text{Xe}^+ [^2P_{3/2}^{\circ}]$ or a $\text{Xe}^+ [^2P_{1/2}^{\circ}]$ state (excited by 1.33 eV [21]) when the first electron is transferred. It has been shown earlier that excitations of the target that do not require a core electron to change its nl value may be as likely as formation of the target in the ground state [22]. The active electron is then transferred to the excited target core $\text{Xe}^+ [^2P_{1/2}^{\circ}]$, with a high probability due to a high density of crossings with $\text{Xe}^{q+}\text{-Xe} [^2P_{1/2}^{\circ}]nl$ channels around R_I . All such states, except $nl=6s, 7s, 6p$, or $5d$, autoionize through relaxation of the core to the $^2P_{3/2}^{\circ}$ state of Xe^+ [23].

We assume a unit probability for electron transfer back to the target at R_I and estimate the absolute cross sections to be

$$\sigma_I^{\text{mod}} = 2\pi \sum \int_{R_2}^{R_I} [1 - p(b, R_1^I)] b db, \quad (2)$$

where p is the Landau-Zener probability for the crossing at R_1^I and the sum is taken over all channels with $R_I > R_2$. Since there is a quasicontinuum of such channels and since the probability of populating a certain channel is peaked at $b = R_I$, we assume that each channel only gets its contribution from a single impact parameter b . Then the cross section becomes

$$\sigma_I^{\text{mod}} = 2\pi \int [1 - p(R_I, R_1^I)] R_I dR_I, \quad (3)$$

where the integration is from R_2 to the maximum $R_I = (q-1)/I_1$. In reality several impact parameters contribute for each channel. Thus, this tends towards an underestimation of the cross section, while the assumed unit probability of electron transfer back to the target at

R_I acts in the opposite direction. We have further not included the probability (statistical weight $\frac{1}{3}$) for leaving the target in the core-excited state at the R_1^I transition. In Fig. 1, we show σ_I^{mod} multiplied by a factor of 4 and find excellent agreement with the experimental data. The model cross section has the functional form $\sigma_I^{\text{mod}} \sim (q-16)^2$, in agreement with our experimental findings. The model further implies that the cross sections for ionization and excitation (population of $[^2P_{3/2}^{\circ}]nl$ states) should be of similar magnitude and that the velocity dependences should be weak in the adiabatic region. The present ionization mechanism is unique for targets with p^6 cores, and we note that our preliminary $\text{Xe}^{q+}\text{-Ar}$ data for $v=0.034\sqrt{q}$ a.u. also show indications of ionization.

In this Rapid Communication we have presented the discovery of a strong onset of ionization in *slow* $\text{Xe}^{q+}\text{-Xe}$ collisions in the charge-state region $15 \leq q \leq 37$. The collision velocity is well below the characteristic one at which ionization without accompanying electron capture is virtually prohibited from a classical point of view [2]. We suggest that the ionization process is mediated by a truncated capture event, leading to population of autoionizing, core excited, neutral Xe states. Although crude, the model readily explains the threshold in q and the approximate q^2 increase of the ionization cross section at high projectile charge states.

We are grateful to Leif Liljeby and Åke Engström for providing the beam. Nils Elander and Reinhold Schuch are acknowledged for stimulating discussions. This work was supported by the Swedish National Research Council.

-
- * Present address: Institute of Physics, Pedagogical University 25 509 Kielce, Poland.
- [1] E. Rutherford, *Philos. Mag.* **47**, 277 (1924).
 - [2] N. Bohr and J. Lindhard, *K. Dan. Vidensk. Selsk. Mat. Fys. Medd.* **28**, No. 7 (1954).
 - [3] P. Hvelplund, H.K. Haugen, and H. Knudsen, *Phys. Rev. A* **22**, 1930 (1980).
 - [4] H. Cederquist *et al.*, *Phys. Rev. A* **46**, 2592 (1992).
 - [5] H. Cederquist *et al.*, in *Proceedings of the Seventeenth International Conference on the Physics of Electronic and Atomic Collisions, Brisbane, Australia, 1991*, edited by I.E. McCarthy, W.R. MacGillivray, and M.C. Standage (IOP Publishing Ltd., Bristol, 1992), p. 391.
 - [6] L. Liljeby and Å. Engström, in *International Symposium on Electron Beam Ion Sources and Their Applications*, Proceedings of the International Symposium, Brookhaven National Laboratory, Upton NY, edited by Ady Herscovitch, AIP Conf. Proc. No. 188, (AIP, New York, 1989), p. 27.
 - [7] P. Hvelplund, A. Bárány, H. Cederquist, and J.O.K. Pedersen, *J. Phys. B* **20**, 2515 (1987).
 - [8] D.C. Griffin *Phys. Scr.* **T28**, 17 (1989).
 - [9] E.H. Nielsen *et al.* *J. Phys. B* **18**, 1789 (1985).
 - [10] E. Justiniano *et al.*, *Phys. Rev. A* **29**, 1088 (1984).
 - [11] I.I. Sobelman, *Atomic Spectra and Radiative Transitions*, edited by V.I. Goldanski, R. Gomer, F.P. Schäfer, and J.P. Toennies (Springer-Verlag, Berlin, 1979).
 - [12] R. Ali *et al.* (unpublished).
 - [13] J.P. Giese, in *Abstracts for the Twelfth International Conference on the Application of Accelerators in Research and Industry, Denton, 1992*, edited by Jerome L. Duggan and I.L. Morgan (University of North Texas, Denton, 1992).
 - [14] R.K. Janev and L.P. Presnyakov, *J. Phys. B* **13**, 4233 (1981).
 - [15] A. Bárány and S. Ovchinnikov, *Phys. Scr.* (to be published).
 - [16] A. Bárány *et al.*, *Nucl. Instrum. Methods, Phys. Res. B* **9**, 397 (1985).
 - [17] A. Niehaus, *J. Phys. B* **19**, 2925 (1986).
 - [18] R.E. Olson and A. Salop, *Phys. Rev. A* **14**, 579 (1976).
 - [19] R. Mann *et al.* *Phys. Rev. Lett.* **49**, 1329 (1982).
 - [20] H. Tawara *et al.*, *J. Phys. B* **18**, 337 (1985).
 - [21] C.E. Moore, *Atomic Energy Levels*, Circ. Natl. Bur. Stand. (U.S.) No. 467 (U.S. GPO Washington, DC, 1958), Vol. 3.
 - [22] H. Cederquist *et al.*, *J. Phys. B* **18**, 3951 (1985).
 - [23] J.Z. Wu *et al.* *Phys. Rev. A* **42**, 1350 (1990).